# Optimizing Raman Ladder Climbing: Theory and Application in $Na_2$

**Bo Y. Chang, Ignacio R. Solá,* and Jesús Santamaría**

*Departamento de Química Física I, Universidad Complutense, 28040 Madrid, Spain*

*Received: March 22, 2001; In Final Form: June 22, 2001*

The theory of vibrational ladder climbing excitation by coherent stimulated nonresonant Raman using chirped laser pulses is developed. We analytically obtain the conditions for inverting the population to a final preselected vibrational state and the restrictions that apply in the linear chirp regime. By controlling both the shape of the laser pulses and the chirp profile, the ladder climbing process can be accelerated without reducing the yield of the selective excitation. Numerical results are presented for selection of moderately excited vibrational levels in $Na_2$, where the important contribution of several excited electronic states is also clarified.

## I. Introduction

Exciting molecules in specific high vibrational states has been a long-sought goal, both for a better understanding of the spectroscopic properties of the molecule and for igniting some unimolecular (bond breaking) or bimolecular (reactant preparing) reactions.[1] In molecules with a permanent dipole moment, infrared (IR) laser pulses have been used to pump the vibrational energy. By multiphoton IR processes, it has been possible to excite single modes in regions of high anharmonicity and to observe the subsequent intramolecular vibrational relaxation (IVR).[2] However, due to the very weak transition dipole moments between the ground and high vibrational eigenstates, population inversion is unlikely to succeed. For coherent interactions, the minimum time for population inversion (defining the so-called $\pi$ pulses) is given by $\pi$ times the inverse of the Rabi frequency, $\Omega_{0v}(t) = \mu_{0v}E(t)/\hbar$, where $E(t)$ is the pulse envelope and $\mu_{0v} = \langle\psi_v|\mu|\psi_0\rangle$ is the transition dipole moment between the initial ($\psi_0$) and final ($\psi_v$) vibrational eigenfunctions. For very weak transitions, $\mu_{0v} \ll 1$, and therefore population inversion requires long pulses, with the onset of decoherent and nonradiative processes, or very strong laser sources, usually implying competition between several multiphoton routes, if not directly ionizing the molecule.[3]

A possibility proposed by Manz and colleagues[4] is to fraction the overall transition into several sequential steps, each of which is driven by a proper $\pi$ pulse. The limit of this strategy is to use one $\pi$ pulse for every single quantum step excitation $v \rightarrow v + 1$. The population then follows a pattern equivalent to climbing a ladder one step after another, which takes advantage of the (usually) larger transition dipole moments involved between adjacent vibrational states, especially in approximately harmonic potentials. Nevertheless, the overall sequence of $(v - 1)\pi$ pulses is both experimentally difficult to prepare and moreover poorly robust, since the yield of each step is very sensitive to frequency, time, and intensity variations, and the overall yield is the product of the yields of every step. This also explains the inability of optimal control algorithms to obtain this kind of solution, when not properly biased.[5] Chelkowski et al.[6] and Guerin[7] showed the way to circumvent the problem using a single pulse with slowly varying frequency, adapted to the anharmonicity of the potential. The pulse duration must be at least as long as the whole sequence of $(v - 1)\pi$ pulses and the intensity stronger than the intensity of each one. For sufficiently intense pulses, the population can be adiabatically transferred from the initial state up to dissociation with 100% efficiency at least in principle. The method is both robust and not especially difficult to implement in the laboratory with state-of-the-art technology.[8]

For molecules without a permanent dipole moment, the ladder climbing method can be implemented using nonresonant stimulated coherent Raman.[9−12] In this case, either the pump or the Stokes or both pulses must be chirped. The detuning with respect to excited electronic states is required in order to avoid absorption. Although there are a number of schemes which make use of resonant Raman transitions, such as stimulated Raman adiabatic passage (STIRAP)[13] or stimulated emission pumping (SEP),[14] the Raman ladder climbing is an alternative method especially suited for dissociation or high vibrational energy excitation, since it benefits from the larger effective two-photon transition dipole moments between adjacent vibrational levels.

In this paper, we develop a general theory of Raman ladder climbing deriving the required conditions for the sequential inversion of population between adjacent levels and obtaining the minimum time for the final excitation of a single, selected vibrational level. We demonstrate the important contribution of highly excited electronic states and the possibility of improving the yield of the process by a suitable election of the laser amplitude and chirp profiles. The validity of the theoretical results is numerically tested showing the efficiency of the Raman ladder climbing method applied to the selective excitation of vibrational states of a nonrotating sodium dimer. In section 2, we present the molecular model and calculate the effective Raman Rabi frequencies. In section 3, we develop the theory of optimal Raman ladder climbing, which is numerically tested in section 4. Section 5 is the conclusion.

## II. Model for Nonresonant Raman in $Na_2$

In Raman ladder climbing, the system is exposed to the action of two fully overlapping lasers, the pump $E_p(t)$, and the Stokes $E_s(t)$ pulses. The pulses have the same amplitude, and the frequency of the pump is negatively chirped; that is, its carrier frequency smoothly decreases. The same results can be obtained by positively chirping the frequency of the Stokes pulse or chirping both.

* E-mail: ignacio@tchiko.quim.ucm.es.

10.1021/jp011077s CCC: $20.00 
Published on Web 09/06/2001

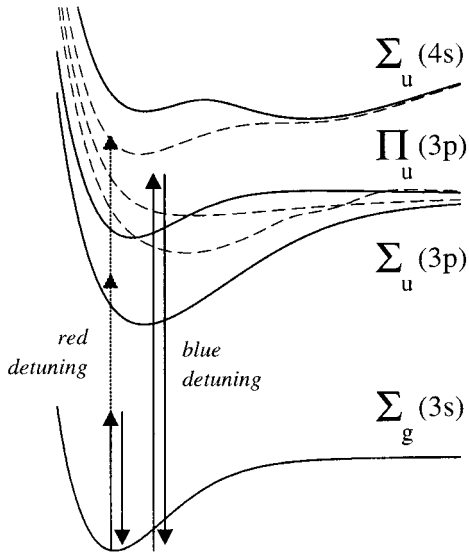


**Figure 1.** First electronic potentials of the $Na_2$ dimer. Solid line are the potentials that can contribute to the Raman process. The remaining potentials are in dashed lines. Also shown are the frequencies of the pump and Stokes pulses used in the calculations of the paper, defining the so-called red detuning and blue detuning cases.

Even in simple diatomic molecules such as $Na_2$, for a quantitative prediction of the dynamics driven by nonresonant pulses, we have to take into account the contribution of several electronic states. In Figure 1, we show the first singlet electronic states of the $Na_2$ molecule.[15] For the nonresonant Raman transition only antisymmetric "u" states [mainly $^1\Sigma_u(3p)$, $^1\Pi_u(3p)$, and $^1\Sigma_u(4s)$] can contribute. We have basically considered calculations at two different wavelengths: $\omega_1 \approx 8933$ cm$^{-1}$ (the red detuning case) and $\omega_1 \approx 24\,296$ cm$^{-1}$ (the blue detuning case). The wavelengths were chosen to avoid competition of other multiphoton processes. As Figure 1 shows, excitation of antisymmetric electronic states by absorption of an odd number of photons, or to symmetric electronic states by absorption of an even number of photons, are all nonresonant and very unlikely for the wavelengths considered. The contribution of $2 + 2$ or $3 + 3$ hyper-Raman processes is also negligible. In this case, the time-dependent Schrödinger equation (TDSE) can be written as

$$i\hbar\begin{pmatrix}\dot{\psi}_1(x,t)\\ \dot{\psi}_2(x,t)\\ \dot{\psi}_3(x,t)\\ \dot{\psi}_4(x,t)\end{pmatrix} = \begin{pmatrix}T+V_1(x) & -\mu_{12}(x)E(t) & -\mu_{13}(x)E(t) & -\mu_{14}(x)E(t)\\ -\mu_{12}(x)E(t) & T+V_2(x) & 0 & 0\\ -\mu_{13}(x)E(t) & 0 & T+V_3(x) & 0\\ -\mu_{14}(x)E(t) & 0 & 0 & T+V_4(x)\end{pmatrix} \times \begin{pmatrix}\psi_1(x,t)\\ \psi_2(x,t)\\ \psi_3(x,t)\\ \psi_4(x,t)\end{pmatrix} \quad (1)$$

where $E(t) = E_p(t)\cos[\omega_p(t)t] + E_s(t)\cos[\omega_s(t)t]$, and we only include the coupling between the ground and the first three excited antisymmetric electronic states.

To further analyze the dynamical behavior of the system, we expand the wave function of the system in the basis of the vibronic eigenstates of the coupled electronic states, $|\psi(q, x, t)\rangle = \Sigma_{\alpha=1}^{M}\Sigma_{j=1}^{N} d_j^{(\alpha)}(t)|\varphi_j^{(\alpha)}(x)\otimes|\Xi_\alpha(q;x)\rangle$ (where $M = 4$ in the model that we use for $Na_2$), and obtain the nonrotating time-dependent Schrödinger equation (TDSE) for the vibrational amplitudes,

$$i\dot{d}_j^{(\alpha)}(t) = \omega_j^{(\alpha)} d_j^{(\alpha)} - \sum_{\beta\neq\alpha}^{M}\sum_{k=0}^{N}\{\Omega_{\alpha j,\beta k}^{(p)}(t)\cos[\omega_p(t)t] + \Omega_{\alpha j,\beta k}^{(s)}(t)\cos[\omega_s(t)t]\}d_k^{(\beta)}(t) \quad (2)$$

In eq 2, the pump and Stokes one-photon Rabi frequencies are those of the electronic transitions between the vibronic states, $\Omega_{\alpha j,\beta k}^{(p)/(s)}(t) = \langle\varphi_j^{(\alpha)}\otimes\Xi_\alpha|\mu E_{p/s}(t)|\varphi_k^{(\beta)}\otimes\Xi_\beta\rangle\hbar$, where $E_{p/s}(t)$ refers to either the pump or the Stokes pulse envelopes. The fast oscillatory terms that depend with the carrier frequencies of the pulses $\omega_{p/s}(t)$ are not included in the Rabi frequency definition. The dot indicates a time derivative. The general Schrödinger equation can be simplified assuming that the population in all the excited electronic states is very small, which is a good approximation for nonresonant transitions when the Rabi frequencies of the absorption processes to the excited states are far smaller than the respective detunings. If additionally the Rabi frequencies are smaller than $\omega_p$, $\omega_s$, and $\omega_p - \omega_s$, then the rotating wave approximation (RWA) can be used. Following the method of adiabatic elimination,[10] the equations of motion for all amplitudes of the excited electronic states, $d_j^{(\alpha)}(t)$with $\alpha > 1$, can be formally integrated in terms of the ground-state amplitudes. Then, the TDSE can be simplify to obtain the following effective equations of motion,[16]

$$i\dot{d}_j^{(1)}(t) = (\omega_j^{(1)} - \Omega_R^{(pp)}(j,j,t) - \Omega_R^{(ss)}(j,j,t))d_j^{(1)}(t) - \frac{1}{2}\sum_{k\neq j} e^{i\delta(t)t}\Omega_R^{(ps)}(j,k,t)d_k^{(1)}(t) \quad (3)$$

where the two-photon detuning is $\delta(t) = \omega_p(t) - \omega_s(t)$ if $k > i$ [or $\omega_s(t) - \omega_p(t)$ if $i > k$, assessing the Hermitian symmetry of the Hamiltonian] and the Rabi frequencies $\Omega_R^{(\alpha\beta)}(j, k, t)$ are now two photon effective Raman Rabi frequencies. To simplify the notation, we have included the index as a discrete variable. Now eq 3 only involves the amplitudes of the ground electronic vibrational states, and therefore is a TDSE that models the dynamics under an effective Raman Hamiltonian. The adiabatic elimination is formally equivalent to a second-order perturbation expansion except that the ground amplitudes are not substituted by their initial values in eq 3. In terms of the one-photon Rabi frequencies, the diagonal two-photon effective Raman Rabi frequencies are

$$\Omega_R^{(pp)/(ss)}(j,j,t) = \frac{1}{2}\sum_{\alpha=2m=0}^{M}\sum^{N}\frac{(\Omega_{\alpha m,1j}^{(p)/(s)}(t))^2(\omega_m^{(\alpha)} - \omega_j^{(1)})}{(\omega_m^{(\alpha)} - \omega_j^{(1)})^2 - \omega_{p/s}(t)^2} \quad (4)$$

giving account of the dynamic Stark shifts, whereas the nondiagonal coupling terms are

$$\Omega_R^{(ps)}(j,k,t) = \frac{1}{2}\sum_{\alpha=2m=0}^{M}\sum^{N}\Omega_{\alpha m,1k}^{(p)}(t)\Omega_{\alpha m,1k}^{(s)}(t)\left(\frac{1}{\omega_m^{(\alpha)} - \omega_k^{(1)} - \omega_p(t)} + \frac{1}{\omega_m^{(\alpha)} - \omega_k^{(1)} + \omega_s(t)}\right) \quad (5)$$

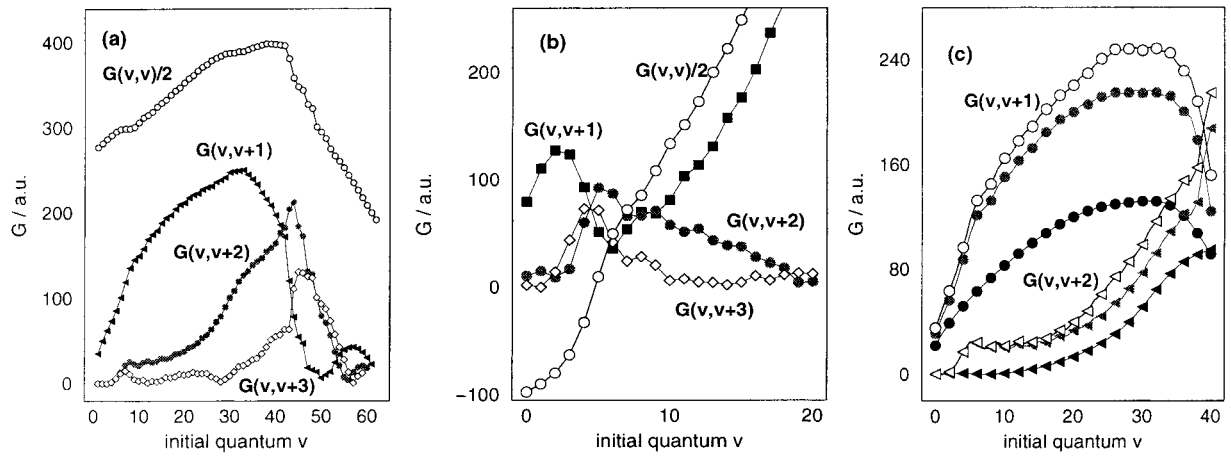


**Figure 2.** Effective Raman transition dipole moments ($G_R(i, j)$) giving account of the Stark shift and sequential ladder climbing couplings. (a) $G_R(i, j)$ calculated for the red detuning case and (b) for the blue detuning case. (c) Calculation done including only the first excited potential or three excited potentials, as in the model proposed in the paper.

with $j \neq k$, which provide the transition amplitudes for the vibrational ladder climbing. The two-photon Rabi frequencies involve a summation over all the ($N$) vibrational levels $\varphi_m^{(\alpha)}(x)$ (with eigenvalues $\omega_m^{(\alpha)}$) of every ($M$) excited electronic state $\alpha$ coupled with the ground state. In our calculations, we limit $M$ to the first three antisymmetric excited electronic states. The effective Raman Rabi frequencies depend on the intensity of the field. Their time dependence comes from the laser profile via the one-photon Rabi frequency, and from the time-dependent detuning in the denominators, which is very slow and can be neglected or expanded as a function of the chirp. Therefore, we can define the effective Raman transition dipole moments (RTM), $G_R(j, k) = \{\Omega_R^{(\alpha\beta)}(j, k, t)\}/\{E_\alpha(t)E_\beta(t)\}$, which only depend on the geometry and energy of the potential energy curves involved, that is, on the Franck−Condon factors and the carrier frequencies of the lasers.

The effective Raman transition dipole moments provide information about the probability of ladder climbing in steps of one vibrational quantum $G_R(j, j + 1)$ (second diagonal of the effective Hamiltonian), two vibrational quanta $G_R(j, j + 2)$ (third diagonal), three vibrational quanta $G_R(j, j + 3)$ (fourth diagonal), and so on. To compute the RTM coefficients, we obtain the eigenstates and eigenvalues of the four electronic potentials by the FGH method[17] using a very extended grid (up to $x = 20$ Å) that faithfully represents the dissociation. The potentials and dipole moments are taken from ab initio calculations of Schmidt.[15]

In Figure 2, we show the coefficients for the first diagonals both in the red and blue detuning cases. The importance of including more than one electronic state in the calculations is made clear in Figure 3, where we compute the RTM including only one, two, or three excited electronic states [$\alpha = 2-4$ in eqs 4 and 5]. It can be seen that the net effect of the potentials adds to the calculation of the RTM, and only the contribution of very off-resonant potentials is negligible. In the red-detuning case, after summing the contribution of the first three excited electronic states, we obtain practically converged results of the RTM at least for the first vibrational levels, but omission of the contribution of any of these potentials [especially $^1\Sigma_u(3p)$ and $^1\Pi_u(3p)$] would imply a gross error in the calculation. In the blue detuning case, we only compute the first 20 RTM because higher vibrational states are in resonance with the lower vibrational states of $^1\Sigma_u(4s)$. Therefore, the denominator of eqs 4 and 5 tends to zero, and the effective Hamiltonian is no longer valid, since absorption to the excited electronic state breaks the

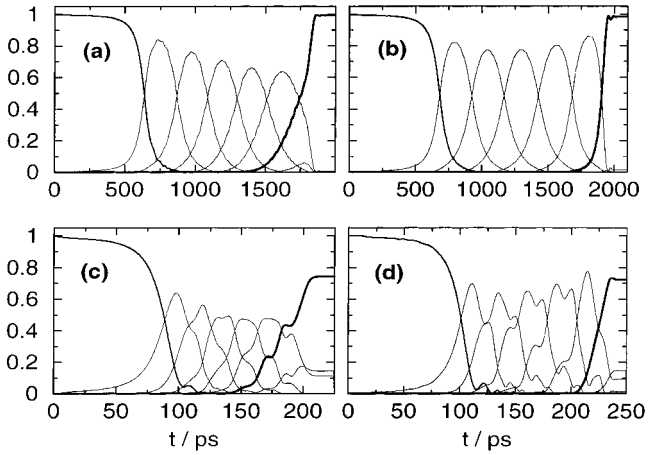


**Figure 3.** Results using constant field and linear chirp lasers, for two different time regimes in the red detuning (a) and (c), and blue detuning (b) and (d) cases. The population of the first vibrational levels is represented showing the selection of $v = 6$ at final times.

assumptions of the model. In the red detuning case, transitions from higher ground vibrational states to $^1\Sigma_u(4s)$ are also possible by three photon absorption. However, by wave packet propagation with the full Hamiltonian (including the four electronic potentials), we have checked that this probability remains very low for the intensities tested in our numerical calculations.

## III. Optimization of Raman Ladder Climbing

Raman ladder climbing is usually implemented for steps of one vibrational quantum because, as seen in Figure 2, the coupling is maximal between sequential vibrational eigenfunctions for the first transitions. Therefore, at the beginning, we choose the carrier frequencies of the pump and Stokes pulses such that the two-photon detuning, $\delta(0) \equiv \omega_p(0) - \omega_s(0)$, should be larger than the frequency of the first transition, $\omega_{01} \equiv \omega_1^{(1)} - \omega_0^{(1)}$. We can define an extra energy such that $\delta(0) = \omega_{01} + \omega_i$. For transitions induced by frequency sweeping, this initial extra energy above the first resonance is required to ensure the full adiabatic passage of population between the coupled levels in the following crossing.[7] Now, negatively chirping the pump frequency, we adapt the detuning to the decreasing energy splitting between adjacent levels (in anharmonic molecules). When both pulses are switched off, if we want to select the $n$th vibrational state, the detuning must be smaller than $\omega_{n,n-1} \equiv \omega_n^{(1)} - \omega_{n-1}^{(1)}$, but larger than $\omega_{n+1,n} \equiv \omega_{n+1}^{(1)} - \omega_n^{(1)}$.

$$\frac{H^{ef}}{\hbar}=\begin{pmatrix} \omega_0^{(1)}-\Omega_R(1,1,t) & -\Omega_R^{(ps)}(1,2,t)/2 & 0 & \cdots \\ -\Omega_R^{(ps)}(1,2,t)/2 & \omega_1^{(1)}-\Omega_R(2,2,t)-\delta(t)-\dot{\delta}(t)\Delta t & -\Omega_R^{(ps)}(2,3,t)/2 & \cdots \\ 0 & -\Omega_R^{(ps)}(2,3,t)/2 & \omega_2^{(1)}-\Omega_R(3,3,t)-2[\delta(t)+\dot{\delta}(t)\Delta t] & \cdots \\ \vdots & \vdots & \vdots & \ddots \end{pmatrix} \quad (6)$$

Therefore, the pulse must be tailored in a controlled way in order to select a single vibrational eigenfunction, especially for short pulses and higher vibrational states.

To proceed with the theory, we will now assume that we can neglect the effective couplings between nonadjacent levels. This is a very good approximation for the first levels, but, as Figure 2 reveals, for higher vibrational levels the two- or even three-step amplitudes can be far larger than the one-step amplitudes. Then, the respective Rabi frequencies might exceed the detunings, which are decreasing due to the anharmonicity, stopping or branching the one-stepladder climbing.[18] If all couplings except the one-step are set to zero, the effective Hamiltonian has a three-diagonal form. Then, by a suitable unitary transformation we obtain eq 6, where the diagonal Raman effective coupling includes the contribution from both the pump and Stokes pulses. Since we only consider synchronous pulses, such that the pump and Stokes pulse shapes are the same, $E_p(t) = E_s(t) = E(t)$, we will define a global Stark shift coefficient, $G_R(j, j) = G_R^{(pp)}(j, j) + G_R^{(ss)}(j, j)$, such that $\Omega_R(j, j, t) = G_R(j, j)E(t)^2$.

The Hamiltonian in eq 6 ensures the sequential crossing between adjacent vibrational levels. In the diabatic states representation, when consecutive diagonal matrix elements of the Hamiltonian are equal, $H_{j+1,j+1}^{ef}(t_c^{(j)}) = H_{j,j}^{ef}(t_c^{(j)})$, there will be a crossing between the vibrational levels $j$ and $j + 1$. This implies that

$$\omega_{j+1,j} - [\delta(t_c^{(j)}) - \delta(t_c^{(j)})t_c^{(j)}] - [\Omega_R(j+1, j+1, t_c^{(j)}) - \Omega_R(j, j, t_c^{(j)})] = 0 \quad (7)$$

We can define a chirp function (or rate of frequency change) such that

$$\dot{\delta}(t) \equiv \omega_p(t) - \omega_s(t) = \delta(0) - \int_0^t dt'\lambda(t') \quad (8)$$

The instantaneous chirp is then $\dot{\delta}(t) = \lambda(t)$, and the average chirp is $\lambda_{av}(t) = \int_0^t dt'\lambda(t')/t$. Then, the time of crossing between $j$ and $j + 1$ is

$$t_c^{(j)} = \frac{[\delta(0) - \omega_{j+1,j}] + [\Omega_R(j+1, j+1, t) - \Omega_R(j, j, t)]}{\lambda_{av} + \lambda} \quad (9)$$

For most diatomic molecules (particularly in the lowest vibrational levels), the second difference between adjacent vibrational levels is constant. Therefore, $\omega_{j+1,j} \approx \omega_f - 2j\chi$, where $\omega_f$ is the fundamental frequency and $\chi$ is the anharmonicity constant. Making $\delta(0) = \omega_{01} + \omega_i = \omega_f - 2\chi + \omega_i$, the time for the first crossing (between the ground and the first excited state) will be

$$t_c^{(0)} = [\omega_i + \Omega_R(1, 1, t) - \Omega_R(0, 0, t)]/(\lambda_{av} + \lambda) \quad (10)$$

The next crossing, between $v = 1$ and $v = 2$, requires an additional time of

$$t_{12} = [2\chi + \Omega_R(2, 2, t) - \Omega_R(1, 1, t)]/(\lambda_{av} + \lambda) \quad (11)$$

For the final selection of $v = j + 1$,

$$t_c^{(j)} = [\omega_i + 2j\chi + \Omega_R(j+1, j+1, t) - \Omega_R(j, j, t)]/(\lambda_{av} + \lambda) = t_c^{(0)} + t_{12} + t_{23} + ... + t_{j,j+1} \quad (12)$$

where the last step requires an additional time of

$$t_{j,j+1} = [2\chi + \Omega_R(j+1, j+1, t) - \Omega_R(j, j, t)]/(\lambda_{av} + \lambda) \quad (13)$$

Therefore, the time for each transition depends on the anharmonicity and the difference between the Raman amplitudes $G_R(j + 1, j + 1) - G_R(j, j)$. Control over this parameter can be exerted directly by the chirp function (through the average and instantaneous chirp rates), and indirectly by the field shape $E(t)$, which enters into the diagonal Raman effective couplings. However, for almost harmonic molecules, ladder climbing will be unlikely to succeed, since all the levels cross at the same time.

Each sequential transition can be approximately formulated in terms of a Landau−Zener crossing of limited time duration $t_{j,j+1}$. Since for each time interval we may consider the field to be constant with value $E(t_{j,j+1})$, the Landau−Zener formula provides the asymptotic probability for the crossing as

$$P_{j+1}(t \rightarrow \infty) = 1 - \exp(-\pi\Omega_R(j, j+1, t_{j,j+1})^2/2(\lambda_{av} + \lambda)) \quad (14)$$

If the exponent is large, the probability $P_{j+1}(t \rightarrow \infty)$ will be practically unity, and therefore $P_j(t \rightarrow \infty)$ will be zero. In the adiabatic representation, the crossing is not limited to a single moment of time, and it requires some time for the transition to be effective. Actually, the Landau−Zener formula (eq 14) only provides the result in the diabatic representation for infinite time. However, for all practical means, we can define from eq 14 an approximate time required for the Landau−Zener type crossing to be effective[19] as

$$t_{LZ} \sim \Omega_R(j, j+1, t_{j,j+1})/2(\lambda_{av} + \lambda) \quad (15)$$

This time must be shorter than the time that we dispose for the transition, $t_{j,j+1} = 2\chi/(\lambda_{av} + \lambda)$. Therefore, for full crossing, two conditions must be satisfied at the same time:

$$\text{Condition 1: } \Omega_R(j, j+1, t_{j,j+1})^2 \geq 2(\lambda_{av} + \lambda) \quad (16)$$

and

$$\text{Condition 2: } \Omega_R(j, j+1, t_{j,j+1}) \leq 2\chi \quad (17)$$

If the first condition is not satisfied, then the adiabatic passage is broken, and some population will remain in intermediate levels; if the second condition fails, then during the time interval $t_{j,j+1}$, vibrational levels of energy higher than j+1 will be excited before the population is fully transferred to $j + 1$. Therefore, condition 2 corresponds to keeping the order of the sequence by separating the Landau−Zener crossings. The time separation of the sequential crossings is solely guaranteed by the energy criterion in eq 17. From the theoretical point of view, both

conditions justify in principle the validity of the Landau−Zener model. However, it is also possible to extent further the analysis when nonadiabatic couplings contribute to the final yield of the transition.[20]

Since $\Omega_R(j,k)$ depends on $G_R(j,k)$, it is extremely important to consider the net effect of several excited electronic states. For vibrational quanta near $v = 6$, the contribution from the second excited electronic state is oo the same order as the contribution from the first excited state, and $G_R(j, j+1)$ can be about 150% larger than its value computed with just one excited state. Then, if we make calculations of Raman ladder climbing considering only the effect of the first excited electronic state, we would need field amplitudes around 60% larger than those that we actually need.

## IV. Results and Discussion

In Figure 3, we show the results of Raman ladder climbing for the selection of the final vibrational state $v = 6$, in the red and blue detuning cases, for different final times. The calculations were made integrating the TDSE given in eqs 3−5 by a standard procedure.[21] To test the liability of the calculations, we have also integrated the more general Born−Oppenheimer TDSE, without using the RWA and including the ground and the first three electronic antisymmetric states (eq 1). The numerical procedure to solve eq 1 combines a split-operator propagator and a FFT technique to evaluate both the kinetic and potential terms in their diagonal representation. To do so, we diagonalize by a standard procedure the matrix with laser couplings and potential curves at every grid point and instant of time. The wave packets are expanded on a spatial grid of 512 points spanning ∼10 Å, and the time step is fixed to 1 au. Since solving eq 1 is time-consuming, even for a computer, we have simply verified that the reduced Raman Hamiltonian faithfully reproduces the dynamics for both the red and blue detuning cases under the most intense fields probed in our calculations. That is, for the previous laser frequencies, intensities and durations, losses due to absorption to excited electronic states are not important.

We have used fields of constant amplitude $E_0$ except for a short period of switching on and off (∼25 ps) with a linear chirp function for the pump pulse, $\omega_p(t) = \omega_p(0) - \lambda_p t$, whereas the Stokes pulse has fixed carrier frequency $\omega_s(0)$. Then, $\lambda_{av}(t) = \lambda(t) = \lambda_p$, and the time of crossing between two consecutive levels is

$$t_{jj+1} = \frac{\chi}{\lambda_p} + \frac{\Omega_R(j+1, j+1, t) - \Omega_R(j, j, t)}{2\lambda_p} \qquad (18)$$

In the upper plots of Figure 3, we test the performance of the red (a) and blue (b) detuning cases with $\lambda_p = 3.2$ cm$^{-1}$/ns and $E_0 = 1.2$ MV/cm for the red detuning case (a) and $E_0 = 0.87$ MV/cm for the blue detuning case (b). In the lower plots of Figure 3, we use $\lambda_p = 34$ cm$^{-1}$/ns, and $E_0 = 2.1$ MV/cm for the red detuning case (c) and $E_0 = 1.3$ MV/cm for the blue detuning case (d). The parameters were chosen by fixing the chirp rate and finding the field amplitude that provided the best final yield possible.

As can be seen from Figure 3, there are two main differences between the red and blue detuning cases. First, because the RTM are in general larger for the blue detuning, we need lower field intensities in order to have similar two-photon Rabi frequencies. Moreover, since $G_R^{(ps)}(j, j+1)$ decreases for the last transitions before $j = 6$ (noticeable on Figure 2), condition 2 is better accomplished for the last transitions, and therefore for the last steps of the ladder, population inversion is almost perfect. For the red-detuning case, $G_R^{(ps)}(j, j+1)$ are always increasing, and the population inversion is poorer at the last steps. The second main difference stems from the diagonal elements. In the blue detuning case, for the first vibrational quanta, $G_R(j, j)$ increases almost linearly with $j$ (again visible in Figure 2). Therefore, each sequential crossing requires more time than that for the red detuning case, where $G_R(j+1, j+1) \approx G_R(j, j)$.

Since for $Na_2$ the anharmonicity is very small ($\chi \sim 1$ cm$^{-1}$), full population inversion at each crossing implies the use of weak fields according to condition 2 (eq 17). This in turn implies low chirp rates by condition 1 (eq 16) and leads to long times for the final excitation, since the global time is approximately $t_c^{(j)} \approx (\omega_i + 2j\chi)/2\lambda_p$. Therefore, we get the apparent contradiction that although the global frequency swept $\delta(t_c^{(j)})$, is smaller for molecules with low anharmonicity, the global time for complete excitation must be larger.

In $Na_2$, the molecular constraints due to $\chi$ and $G_R^{(ps)}(j, j+1)$ lead to the following limiting parameters for the excitation of $v = 6$: Since the maximum RTM ($G_{max}$) is around 100 au and the field amplitude is constant, condition 2 fixes the maximum field possible as $E_{max} \sim 0.92$ MV/cm (implying intensities close to the GW/cm$^2$). On the other hand, since the minimum RTM ($G_{min}$) is 30 au and the chirp rate is constant, condition 1 fixes the maximum linear chirp rate possible as $\lambda_{max} \sim 4.5$ cm$^{-1}$/ns. This sets a minimum time for full excitation of $v = 6$ around 1 ns. This is in agreement with the numerical calculations, which provide perfect results only for final times longer than 1 ns. The use of larger chirp rates implies shorter final times and larger field amplitudes, at the expense of degrading the final yield. Moreover, the final result is quite sensitive to the exact time and duration of the switching off of the pulse.

In fact, it can be seen that in the constant field and linear chirp regime, the parameters are constrained by the overall structure of the couplings and by the anharmonicity, instead of the molecular parameters at each crossing. Therefore, the field is constrained to be

$$E_0 \leq \sqrt{2\chi/G_{max}} \qquad (19)$$

while the chirp must be

$$\lambda < \left(\chi \frac{G_{min}}{G_{max}}\right)^2 \qquad (20)$$

and the minimum time for excitation of state $n$ depends essentially on

$$t_n > \frac{n}{\chi}\left(\frac{G_{max}}{G_{min}}\right)^2 \qquad (21)$$

To improve the results for ladder climbing at short times, we have to optimize the Raman ladder climbing method. Full optimization requires finding for each crossing interval of $t_{j,j+1}$ the best amplitude $E(t_{j,j+1})$ and chirp profile $\lambda(t_{j,j+1})$. Whereas optimization of the amplitude is straightforward following eq 17, optimization of the chirp requires considering at the same time the effect of both the instantaneous chirp $\lambda(t)$, and the average chirp $\lambda_{av}(t)$. The last one in a sense provides the linear rate. Therefore, for the same field amplitude, if $\lambda(t) < \lambda_{av}(t)$, then the adiabatic transition will be more nearly perfect but it will require more time; if $\lambda(t) > \lambda_{av}(t)$, then the adiabaticity can be spoiled but the transition (thought not perfect) will be faster.

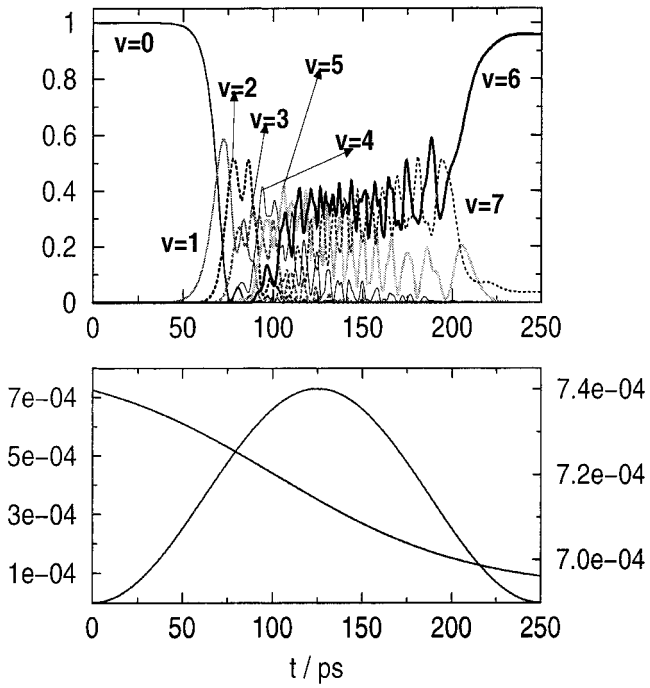


**Figure 4.** Results for the optimal ladder climbing process. In the upper plot, the population of the first vibrational levels is shown. In the lower plot, the shape (left scale) and the nonlinear chirp profile (right scale) of the optimal fields are shown.

Instead of fully optimizing the process, we have chosen a pulse with shape $E(t) = E_0\sin^2(\pi t/\sigma)$ and a nonlinear chirp function (third-order polynomial). We have optimized the chirp for the red detuning case, constraining the final time by the field envelope with $\sigma = 250$ ps. The optimization was carried by line search in the reduced space of three parameters ($E_0$ and two parameters of the chirp function, since we fix the overall frequency swept). Starting from input information from the analytic formulas given in eqs 9, 16, and 17, we select the chirp function that maximizes the yield for a given maximum field $E_0$, and we scan later for different amplitudes.

In Figure 4, we show the results for the populations, optimal field amplitude and optimal chirp. The final yield is better than 95% and therefore implies an improvement of about 30% with respect to the linear chirp and constant amplitude case. In the optimal pulse, the maximum amplitude, $E_0 = 3.8$ MV/cm, is larger than those obtained in the previous constant field cases. For this amplitude, condition 1 is obviously satisfied, ensuring full adiabatic passage, but condition 2 is not. Therefore, the sequential crossings follow without full population inversion, as Figure 4 reveals. Nevertheless, it is important to notice that although the population is flowing to a higher level before it reaches completely each state, the overall population passage is not broken. In other words, the ladder climbing is obscured by the dynamics, but the excitation upward proceeds.

The behavior of the chirp function is also easy to understand. Both at initial and final times, it deviates from linearity with $\lambda(t) < \lambda_{av}(t)$, compensating for the smaller amplitude of the field. At initial times, this is actually not very important, since the process starts far from the resonance of the first crossing. At final times, on the contrary, it is crucial. Since the field is decreasing, eq 17 is now satisfied. There is time to invert completely the population before exciting the next level. We need now to lower the chirp in order not to break the adiabatic passage. When both conditions are satisfied, the yield of population inversion to a single level is almost perfect. Of course, the price to pay is that the last transition expends almost half the time of the overall process.

## V. Conclusions

We have shown that Raman ladder climbing can be an effective way to invert the vibrational population in molecules without permanent dipole moment, such as $Na_2$. We derived the conditions that the pulses must meet in order to sequentially excite vibrational levels up to a final selected state both efficiently and in a robust way, without considering rotational effects.

For a specific molecule, we must first select the carrier frequencies to avoid absorption to highly excited electronic states. For $Na_2$, we propose two different experiments: one using small frequencies red detuned from all the excited electronic states, and the other using larger frequencies detuned to the blue of the first two excited electronic states. To compute the effective Raman transition dipole moments, it is essential to consider the effect of several electronic states. Since the effect increases the Rabi frequencies, we need to use lower fields than those that would be expected if the calculation were done with just one electronic excited state. Therefore, the molecular complexity arising from all the excited electronic state helps to improve the results of Raman ladder climbing.

The main constrain for the success of the method comes from the anharmonicity of the molecule. This imposes a maximum field and therefore a maximum possible chirp rate, determining the minimum final time to invert the population to a specific level. For $Na_2$, population inversion to $v = 6$ following a perfect ladder climbing pattern, with linear chirp rates and constant fields, implies pulse durations longer than a nanosecond.

However, Raman ladder climbing can be optimized by choosing specific field amplitudes and chirp profiles for each sequential crossing. We have derived the conditions that the optimal fields should satisfy. The core of the theory of optimal Raman ladder climbing is summarized in eqs 9, 16, and 17, which evaluate the time required for the process and two conditions that must be satisfied, implying adiabatic following (condition 1) and full selective transitions (condition 2). We have used the theory to optimize population inversion to level $v = 6$ using a field with fix pulse shape and nonlinear chirp profile. The optimal results show that condition 1must be satisfied during all of the process, but condition 2 only needs to be satisfied in the last step of the ladder climbing. This conclusion might have important consequences for the excitation of highly excited vibrational states and especially for molecular dissociation, where condition 2 is not restrictive.

In this paper, we have only optimized the chirp profile. For molecules with permanent dipole moment, using DC fields, it is also possible to manipulate the Stark shifts and gain more control. We anticipate that our results could be improved using more complicated chirp and laser profiles adapted to each sequential crossing. Therefore, we believe that Raman ladder climbing can benefit from the most recent advances in the chirping technology to become an important scheme for population inversion to highly excited vibrational states.

**Acknowledgment.** The authors thank Stephane Guérin for very stimulated conversations at the beginning of this project. Financial support from the Dirección General de Investigación Científica y Técnica under Project No. PB98-0843 is gratefully acknowledged.

## References and Notes

(1) Crim, F. F. *J. Phys. Chem.* **1996**, *100*, 12725.

(2) (a) Nesbitt D. J.; Field, R. W. *J. Phys. Chem.* **1996**, *100*, 12735. (b) Quack, M. *Annu. Rev. Phys. Chem.* **1990**, *41*, 839. (c) Lehmann, K. K.; Scoles, G.; Pate, B. H. *Annu. Rev. Phys. Chem.* **1994**, *45*, 241. (d) Uzer, T. *Phys. Rep*. **1991**, *199*, 124.

(3) (a) Keldysh, L. V. *Sov. Phys. JETP* **1965**, *20*, 1307.(b) Corkum, P. B.; Burnett, N. H.; Brunel, F. *Phys. Rev. Lett*. **1989**, *62*, 1259.

(4) (a) Combariza, J. E.; Just, B.; Manz, J.; Paramonov, G. K. *J. Phys. Chem.* **1991**, *95*, 10351. (b) Combariza, J. E.; Manz, J.; Paramonov, G. K. *Faraday Discuss. Chem. Soc*. **1991**, *91*, 358. (c) Korolkov, M. V.; Paramonov, G. K.; Schmidt, B. *J. Chem. Phys.* **1996**, *105*, 1862.

(5) Shen, H.; Dussault, J.; Bandrauk, A. D. *Chem. Phys. Lett.* **1994**, *221*, 498.

(6) (a) Chelkowski, S.; Bandrauk, A. D.; Corkum, P. B. *Phys. Rev. Lett.* **1990**, *65*, 2355. (b) Chelkowski, S.; Bandrauk, A. D. *Chem. Phys. Lett*. **1991**, *186*, 264. (c) Chelkowski, S.; Bandrauk, A. D. *J. Chem. Phys.* **1993**, *99*, 4279.

(7) Guerin, S. *Phys. Rev. A* **1997**, *56*, 1458.

(8) (a) Weiner, A. M.; Heritage, J. P.; Thurston, R. N. *Opt. Lett.* **1986**, *11*, 153. (b) Bardeen, C. J.; Wang, Q.; Shank, C. V. *Phys. Rev. Lett.* **1995**, *75*, 3410. (c) Melinger, J. S.; McMorrow, D.; Hillegas, C.; Warren, W. S. *Phys. Rev. A* **1995**, *51*, 3366. (d) Assion, A.; Baumert, T.; Bergt, M.; Brixner, T.; Kiefer, B.; Seyfried, V.; Strehle, M.; Gerber, G. *Science* **1998**, *282*, 919. (e) Maas, D. J.; Duncan, D. I.; Vrijen, R. B.; van der Zende, W. J.; Noordam, L. D. *Chem. Phys. Lett.* **1998**, *290*, 75.

(9) Chelkowski, S.; Gibson, G. N. *Phys. Rev. A* **1995**, *52*, R3417.

(10) Chelkowski, S.; Bandrauk, A. D. *J. Raman Spectrosc.* **1997**, *28*, 459.

(11) Davis, J. C.; Warren, W. S. *J. Chem. Phys.* **1999**, *110*, 4229.

(12) Légaré, F.; Chelkowski, S.; Bandrauk, A. D. *Chem. Phys. Lett.* **2000**, *328*, 469.

(13) Bergmann, K.; Theuer, H.; Shore, B. W. *Rev. Mod. Phys.* **1998**, *70*, 1003.

(14) Hamilton, C. H.; Kinsey, J. L.; Field, R. W. *Annu. Rev. Phys. Chem.* **1986**, *37*, 493.

(15) Schmidt, I. Ph.D. Dissertation, University of Kaiserslautern, 1987.

(16) Our equations are generalizations of those of Chelkowski et al. (see references 10 and 11) including the effect of several electronic states. The notation is also simplified.

(17) Balint-Kurti, G. G.; Dixon, R. N.; Marston, C. C. *Faraday Trans. Chem. Soc.* **1990**, *86*, 1741.

(18) Chang, B. Y.; Sola, I. R.; Santamaria, J. *Chem. Phys. Lett.* **2001**, 341, in press.

(19) Solá, I. R.; Malinovsky, V. S.; Chang, B. Y.; Santamaría, J.; Bergmann, K. *Phys. Rev. A* **1999**, *59*, 4494.

(20) Légaré, F.; Chelkowski, S.; Bandrauk, A. D. *J. Raman Spectrosc*. **2000**, *31*, 15.

(21) Press: W. H.; Teukolsky, S. A.; Vetterling, W. T.; Flannery, B. P. *Numerical Recipes*, 1st ed.; Cambridge University Press: New York, 1986; Chapter 10.